

Possible groundwater dominance in the subglacial hydrology of ice sheet interiors: example at Dome C, East Antarctica

Brad T. Gooch¹, Sasha P. Carter², Omar Ghattas³, Duncan A. Young¹, and Donald D. Blankenship¹

¹Institute for Geophysics, Jackson School of Geosciences, University of Texas, Austin, 78758, USA

5 ²Institute of Geophysics and Planetary Physics, Scripps Institution of Oceanography, University of California, San Diego, 92037, USA

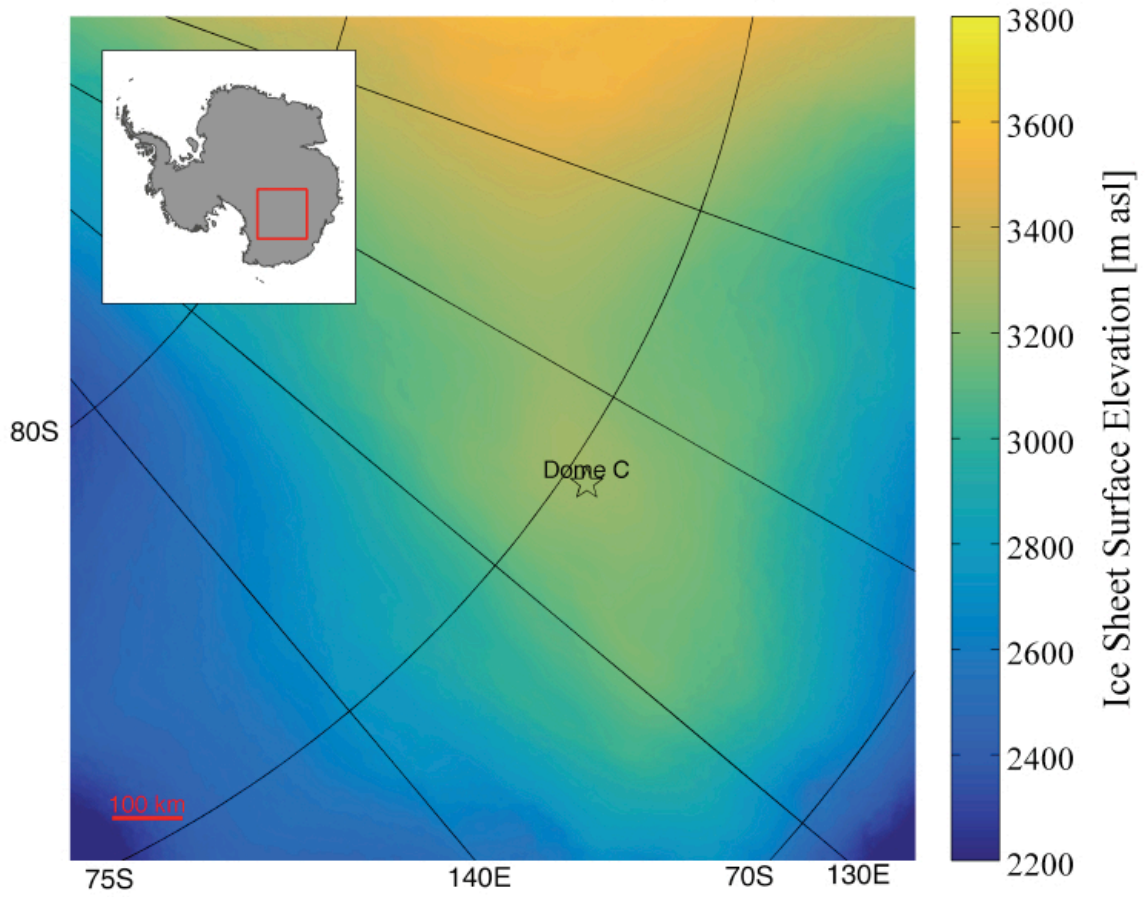
³Institute for Computational Engineering & Sciences, University of Texas, Austin, 78712, USA

Correspondence to: Brad T. Gooch (bgooch@utexas.edu)

10 **Supplement**

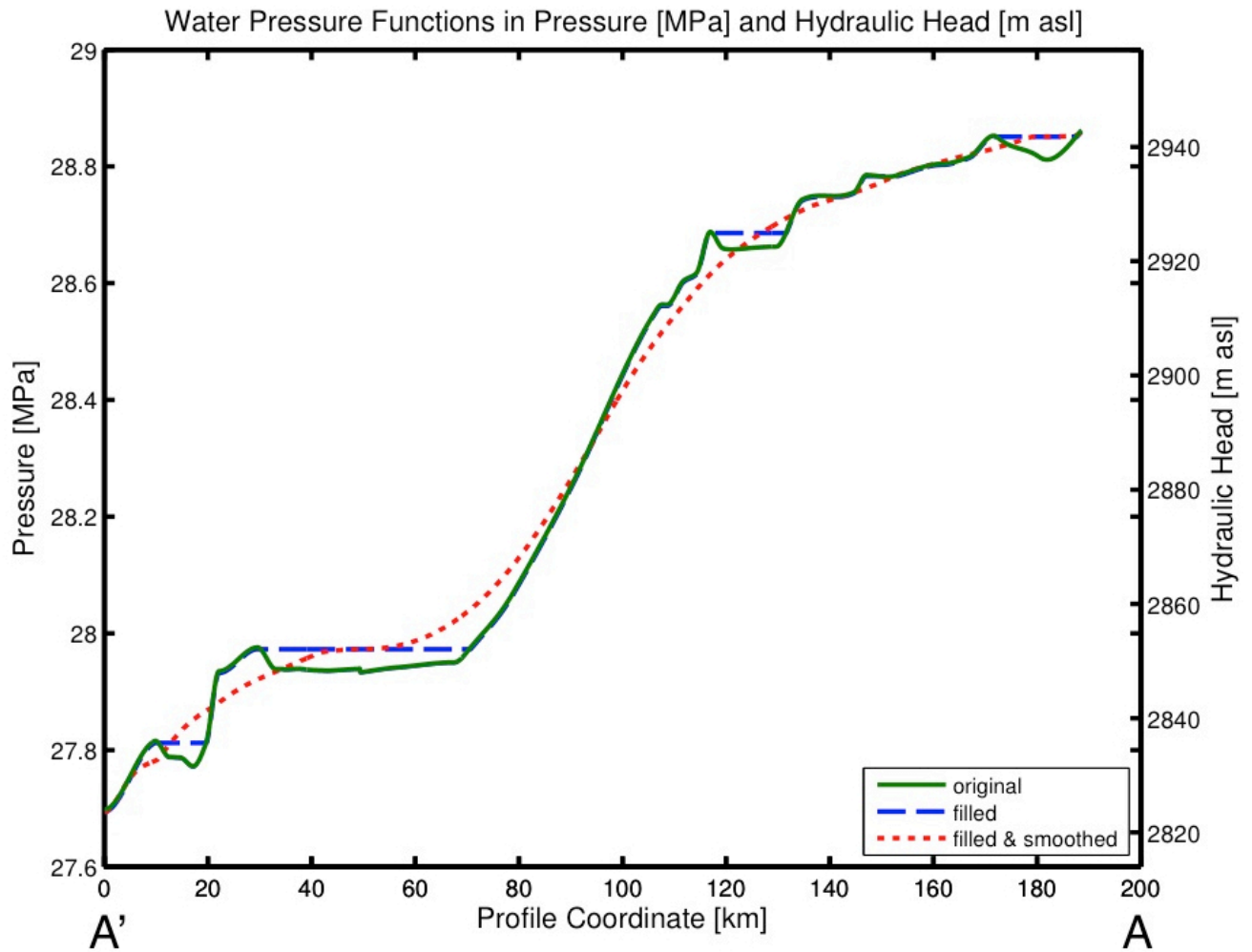
S1 Supplementary Figures

Area used in Fig. 1 Pressure Gradient (∇P) Range Calculation



15

Figure S1. Plot of the area used to calculate the range of pressure gradients (∇P) used in Fig. 1. The surface elevation of the ice sheet uses the Bedmap2 dataset (Fretwell et al., 2013) and shows the location of Dome C in East Antarctica.



20

Figure S2. Plot of the water pressure at the subglacial bed (P_{ws}). Pressure is defined as absolute pressure (MPa) and as hydraulic head (m asl). The original pressure function (solid green line) was filled (dashed blue line) and smoothed (dotted red line) in order to allow a smooth, solvable solution to the 1D water sheet Eq. (2). The location of the profile A-A' is shown in Fig. 3.

25

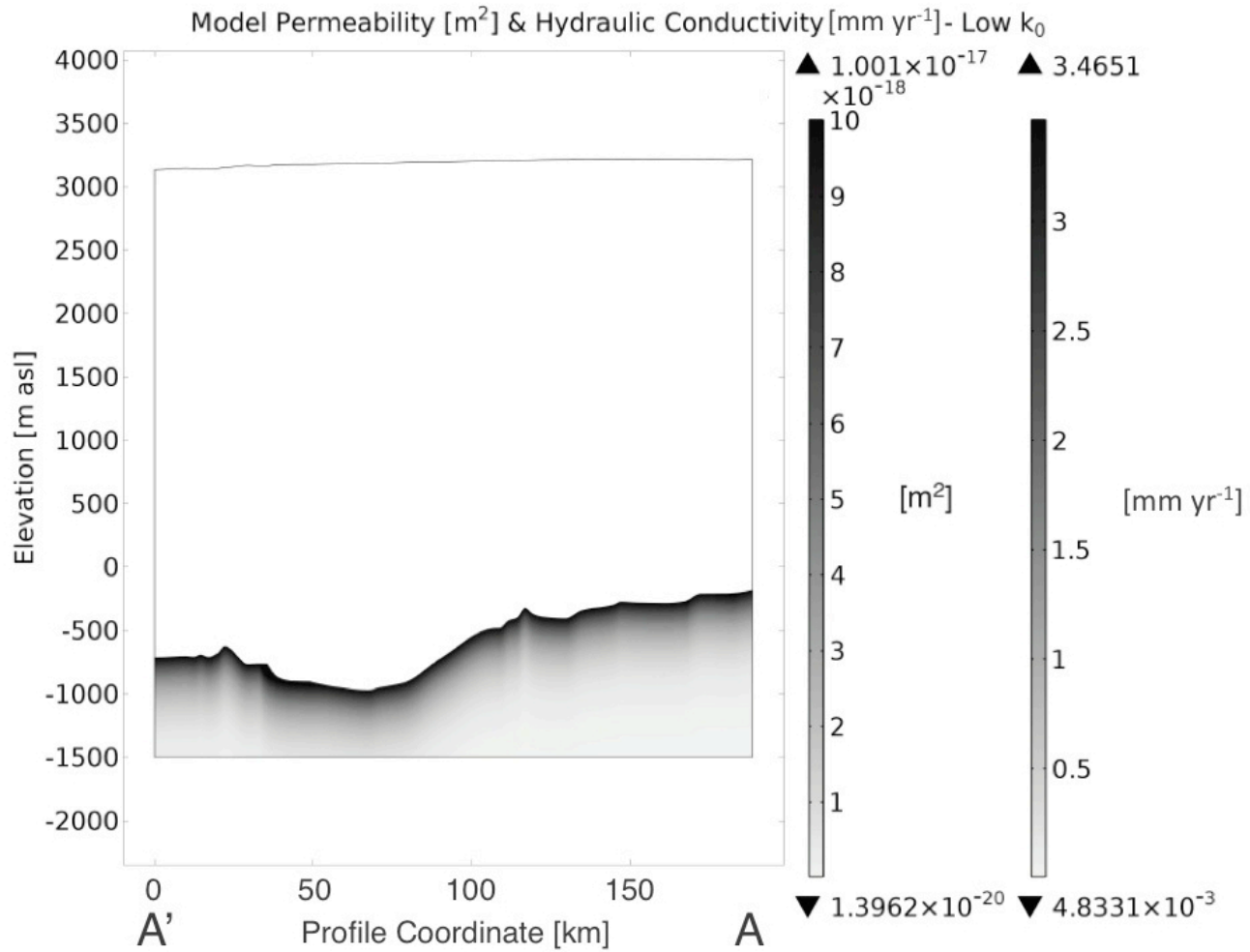


Figure S3. Plot of the permeability and equivalent hydraulic conductivity used in the groundwater subdomain for the lowest k_0 parameterization. As all the parameterizations follow the same exponential law of decreasing permeability with depth, the medium and highest parameterizations are simply 10^3 and 10^6 times the low k_0 (or K_0), respectively. The subglacial lakes are given an isotropic, homogeneous value of k_0 . The location of the profile A-A' is shown in Fig. 3.

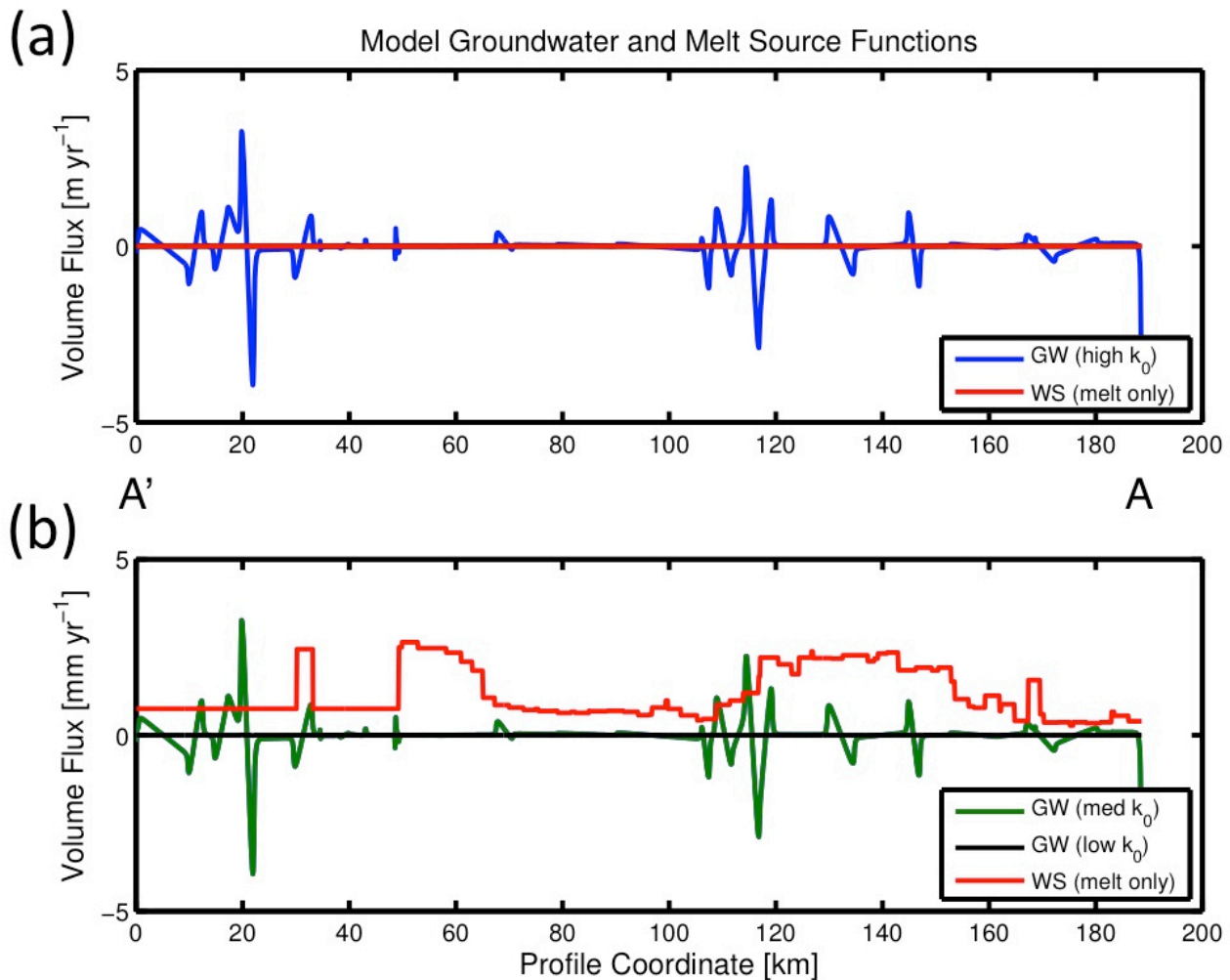


Figure S4. Plot of the groundwater (GW) and basal ice melt rate (WS (Carter et al., 2009b)) water
 35 sources used to calculate the source term (G and \dot{b} , respectively) parameterizations. The location of the
 profile A-A' is shown in Fig. 3. (a) The scale of the top plot is three orders of magnitude greater than
 (b) the bottom (i.e. m yr^{-1} vs. mm yr^{-1}). Note that the various groundwater volume fluxes, q , have
 identical trends but are three (or six if low vs. high) orders of magnitude apart from each other. It is
 important to also note that the groundwater values are derived from the model and the melt rates are
 40 given a priori.

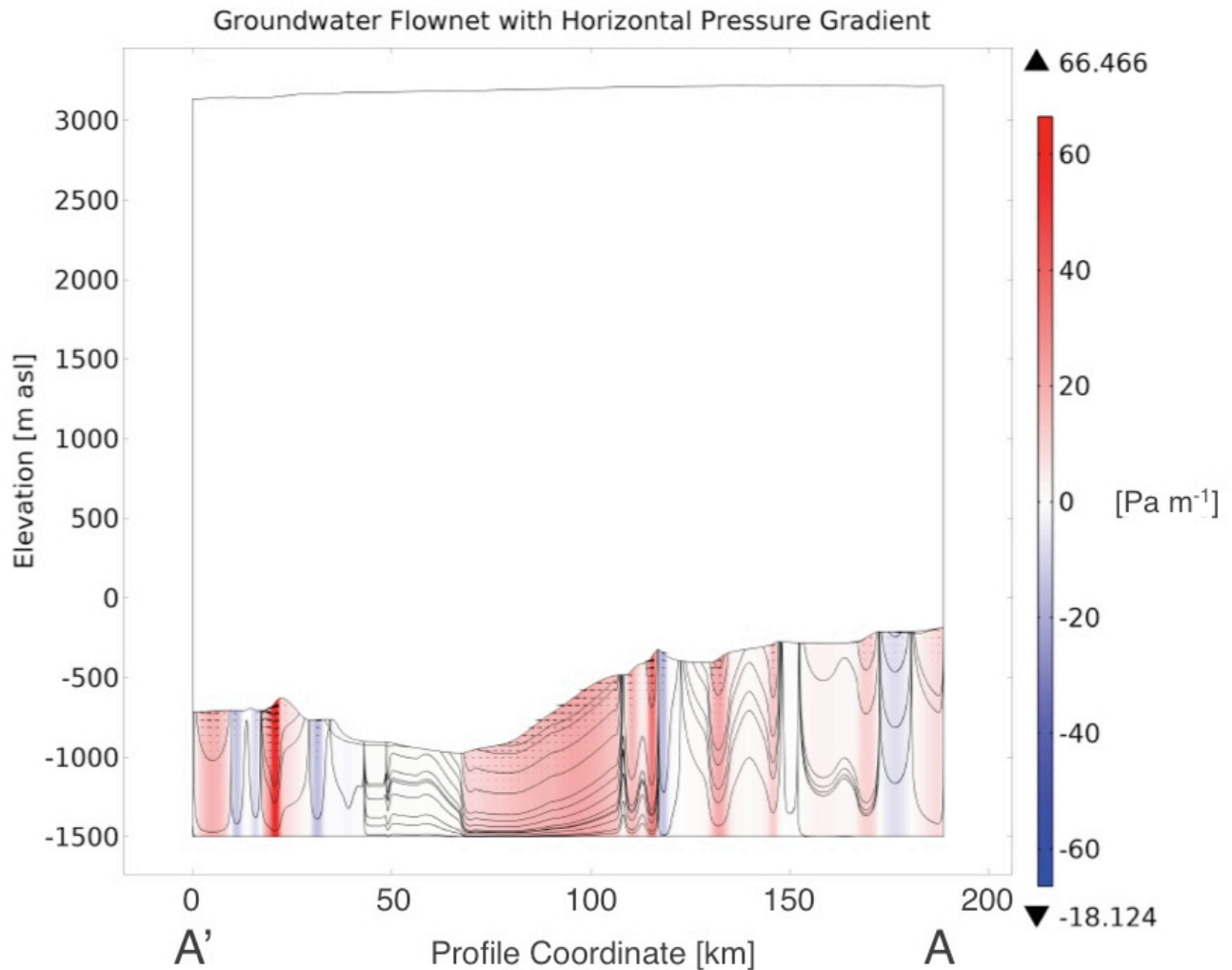


Figure S5. Plot of the modeled subsurface horizontal pressure gradient and the groundwater flownet streamlines (not displayed as equivalent-magnitude stream tubes but via edge point selection) partially shown in Fig. 6 (melt+gw (*high* k_0) model case). Relative magnitude vector arrows are included to demonstrate the flow directions. The three subglacial lakes along the profile are at coordinates 33.2-54.4, 165.2-168.7, and 176.2-188.3 kilometers. Negative pressure gradients (blue) cause water to flow to the right while positive pressure gradients (red) cause flow to the left (i.e. with the downstream subglacial water flow). The location of the profile A-A' is shown in Fig. 3. Note the high level of vertical exaggeration ($\sim 40x$) and that the horizontal flow vector is shown (as arrows); it is the dominant flow direction versus the vertical.

S2 Supplementary References

60 Carter, S. P., Blankenship, D. D., Young, D. A., and Holt, J. W.: Using radar-sounding data to identify the distribution and sources of subglacial water: Application to Dome C, East Antarctica, *J. Glaciol.*, 55(194), 1025–1040, doi:10.3189/002214309790794931, 2009b.

65 Fretwell, P., Pritchard, H. D., Vaughan, D. G., Bamber, J. L., Barrand, N. E., Bell, R., Bianchi, C., Bingham, R. G., Blankenship, D. D., Casassa, G., Catania, G., Callens, D., Conway, H., Cook, A. J., Corr, H. F. J., Damaske, D., Damm, V., Ferraccioli, F., Forsberg, R., Fujita, S., Gim, Y., Gogineni, P., Griggs, J. A., Hindmarsh, R. C. A., Holmlund, P., Holt, J. W., Jacobel, R. W., Jenkins, A., Jokat, W., Jordan, T., King, E. C., Kohler, J., Krabill, W., Riger-Kusk, M., Langley, K. A., Leitchenkov, G., Leuschen, C., Luyendyk, B. P., Matsuoka, K., Mouginot, J., Nitsche, F. O., Nogi, Y., Nost, O. A., Popov, S. V., Rignot, E., Ripplin, D. M., Rivera, A., Roberts, J., Ross, N., Siegert, M. J., Smith, A. M., Steinhage, D., Studinger, M., Sun, B., Tinto, B. K., Welch, B. C., Wilson, D., Young, D. A., Xiangbin, C., and Zirizzotti, A.: Bedmap2: improved ice bed, 70 surface and thickness datasets for Antarctica, *The Cryosphere*, 7, 375–393, doi:10.5194/tc-7-375-2013, 2013.